

# Design, Synthesis, and Optimization of Silver Nanoparticles Using an *Artocarpus heterophyllus* Lam. Leaf Extract and Its Antibacterial Application

Rohankumar R. Chavan<sup>1✉</sup>, Mangesh A. Bhutkar<sup>2</sup>, Somnath D. Bhinge<sup>3</sup>

<sup>1</sup> Rajarambapu College of Pharmacy, Kasegaon, India

<sup>2</sup> Department of Pharmaceutics, Rajarambapu College of Pharmacy, Kasegaon, India

<sup>3</sup> Department of Pharmaceutical Chemistry, Rajarambapu College of Pharmacy, Kasegaon, India

✉ Corresponding author. E-mail: [rohankumar3102@gmail.com](mailto:rohankumar3102@gmail.com)

**Received:** Nov. 28, 2022; **Revised:** Jan. 13, 2023; **Accepted:** Mar. 27, 2023

**Citation:** R.R. Chavan, M.A. Bhutkar, S.D. Bhinge. Design, synthesis, and optimization of silver nanoparticles using an *Artocarpus heterophyllus* Lam. leaf extract and its antibacterial application. *Nano Biomedicine and Engineering*, 2023.

<http://doi.org/10.26599/NBE.2023.9290011>

## Abstract

In this study, the synthesis of nanoparticles and their biological evaluation were carried out. A green synthetic approach synthesized silver nanoparticles (AHAgNPs) using an *Artocarpus heterophyllus* leaf extract. Parameter optimization was performed using Design Expert Ver. 13. The effects of variables like the concentration on the response, particle size, and entrapment efficiency of synthesized AHAgNPs were monitored via analysis of variance. The optimized AgNPs were characterized using ultraviolet–visible spectroscopy and Fourier transform infrared spectroscopy. Scanning electron microscopy and transmission electron microscopy were used to determine the size and shape of nanoparticles. *In vitro*, antioxidant and antimicrobial potential were determined using standard protocols. The optimized nanoparticles were spherical, with an average 100–110 nm particle diameter. The synthesized nanoparticles showed effective antioxidant, antibacterial, and antifungal activity. In addition, AHAgNPs showed increased biological activities.

**Keywords:** antimicrobial; antioxidant; green synthesis; optimization; silver nanoparticles

## Introduction

Nanotechnology involves the modulation of materials at the atomic level, preferably 1–100 nm, by combining physical, chemical, and biological approaches. Because of its increased physical, chemical, and optical properties, converting metals to their nano size is becoming increasingly important [1, 2]. Metal nanoparticles (NPs) with the desired properties are now being created using various physical and chemical techniques that have been thoroughly studied [3, 4]. However, these production

techniques suffer from several drawbacks, as they are time-consuming, expensive, and possibly harmful to the environment and living things [5, 6]. Therefore, there is a clear need for a different, secure, economical, and ecologically responsible way to produce nanoparticles [7, 8]. Inorganic metal ions can be converted into metal NPs by a variety of biocompatible and environmentally acceptable components such as plants, algae [9, 10], and microorganisms (bacteria, fungi, and yeast) [11–13]. Plant metabolites like alkaloids, flavonoids, tannins, phenolic acids, and saponins are primarily involved in

reducing  $\text{Ag}^+$  to  $\text{Ag}^0$  to obtain non-toxic nanosized particles and play an effective role in the capping of the synthesized silver nanoparticles [14]. However, because of their affordable culture costs, one-step fast protocol, safeness, non-toxicity, eco-friendly synthetic approach, and ability to produce enormous production volumes, plants are a more ideal platform for NP synthesis than other biological systems [15, 16].

Emerging infectious diseases (EIDs), particularly those caused by bacteria, have dramatically increased in humans during the past few years. EIDs are infectious diseases whose prevalence has increased over the past ten years and are likely to continue to spread in the future. The prolonged use of antibiotics to treat bacterial infections can harm human health, particularly giving their hepatic and renal toxicities. In addition, there are significant drawbacks to using conventional antibiotics, including their decreased efficacies and the promotion of antibiotic-resistant bacterial strains. One of the key causes of drug resistance is widespread antibiotic usage, gene mutation, and bacterial biofilm production [17–19].

*Artocarpus heterophyllus* Lam. belongs to the Moraceae family, locally known as “Ceylon jack tree or jackfruit”, a yearly fruit plant with a tall and sturdy woody tree [20, 21]. This fruit plant grows in wild tropical forests, especially in India. It is also found in African and South American countries in warm and humid areas [22–24]. Traditionally, this plant has been used widely as a folk medicine for illness, boils, wounds, and skin diseases [25]. *A. heterophyllus* Lam. has anti-inflammatory [26], antifungal [27], antidiabetic [28], antibacterial [29], and antioxidant [30–32] properties as portrayed in various Indian traditional medicine texts [33].

Literature surveys have revealed that efforts have yet to be made to optimize silver NP synthesis using *A. heterophyllus* leaf extract. Since synthesizing such metal nanoparticles involves optimizing the main influencing factors on nanoparticle synthesis, the design of experiments (DoE) was carried out in this work. Currently, the DoE approach is rigorously used in various fields of science, such as analytical chemistry and formulation development, for optimization purposes [34–42]. Optimizing important synthesis parameters was done using Design Expert (Ver.13). Therefore, the aim of the proposed study is (i) the design, synthesis, and optimization of silver

NPs (AHAgNPs) using an *A. heterophyllus* leaf (AHL) extract, (ii) the physicochemical characterization of biosynthesized AHAgNPs, which was done by using ultraviolet–visible (UV–Vis) spectroscopy, X-ray diffraction (XRD), Fourier transform infrared (FT-IR), scanning electron microscopy (SEM), and transmission electron microscopy (TEM), and (iii) the potential antioxidant and antimicrobial roles of produced AHAgNPs, which were all explored to assess their biomedical importance.

## Materials and Methods

### Plant sampling, identification, and extract collection

Leaves of *A. heterophyllus* (family: Moraceae) were collected from Morgiri (Patan) Dist-Satara (MS), India, during August and September 2021, and were identified by Dr. Vinod B. Shimpale from Department of Botany, The New College Kolhapur and deposited in the herbarium with deposition number B01. The shade-dried leaf material was extracted with methanol for 24 h using a soxhlet extraction apparatus and repeated thrice. First, the extract was collected and filtered through filter paper (Whatman No. 1) and concentrated each time using a rotary evaporator (Heidolph, Hei-VAP Core). Then, the crude methanolic extract was used to synthesize nanoparticles and pharmacological activity.

### Chemicals

Analytical-grade chemicals were used for the study. Media and other microbiological accessories were obtained from Himedia. Silver nitrate, 2,2-diphenyl-2-picryl hydrazine hydrate (DPPH), gallic acid, phloroglucinol, and ascorbic acid were obtained from Research Laboratory, Mumbai, Maharashtra.

### Microorganisms used

The test microorganisms used in this study were *Staphylococcus aureus* ATCC 6538, *Bacillus subtilis* ATCC 6051, *Bacillus cereus* ATCC 10987, *Escherichia coli* ATCC 8739, and *Aspergillus Niger* ATCC 16880, which were obtained from the National Collection of Industrial Microorganisms Pune (MS), India.

### Biogenic synthesis of silver nanoparticles

A crude extract of AHL was used for the synthesis of

AHAgNPs, and silver nitrate was the source of silver according to the method described by Refs. [43, 44] with slight modifications. Furthermore, the most important parameters, like the concentrations of  $\text{AgNO}_3$  ( $\mu\text{g/mL}$ ) and the extract ( $\mu\text{g/mL}$ ), were optimized by Design Expert Ver. 13 (Stat-Ease Inc., Minneapolis, MN, USA). The reaction mixture was incubated for 3–4 h at room temperature. Nanoparticle synthesis was observed by the naked eye, focusing on the change in color from light green to dark brown, and analyzed by UV–Vis spectroscopy (JASCO 1800). Finally, the silver nanoparticles were purified through cooling centrifugation at 10 000 r/min for 25–30 min and dried in a vacuum chamber for 24 h at 35 °C.

### ***In silico* parameter optimization**

A two-factor and three-level full factorial design was created and entirely randomized to analyze all possible combinations of all components at all levels. For this purpose, Design Expert Ver. 13.0 was used to optimize the conditions [45, 46]. Two significant factors, i.e.,  $\text{AgNO}_3$  concentration ( $\mu\text{g/mL}$ ) and AHL extract concentration ( $\mu\text{g/mL}$ ), were optimized, taken as independent variables at three contrast levels with minimum and maximum values for each. Nine experimental trials were designed with the given experimental design, as shown in Table 1. Two vital factors, the particle size (nm) and entrapment efficiency (%) of biosynthesized AHAgNPs, were interpreted as responses. The obtained data were further used to perform mathematical evaluations; the quadratic second order was selected for analysis of variance (ANOVA) testing; the predicted  $R^2$  and the interaction between two independent variables were

**Table 1** Factorial batches A1–A9 of silver nanoparticles, entrapment efficiency, and particle size

Batch	Extract ( $\mu\text{g/mL}$ )	$\text{AgNO}_3$ ( $\mu\text{g/mL}$ )	Particle size (nm)	Entrapment efficiency (%)
A1	5.5	5.5	110.5	92.47
A2	5.5	1	108.3	89.6
A3	1	5.5	104.3	85.2
A4	10	1	112.5	95.48
A5	10	10	115.4	98.79
A6	5.5	10	112.5	94.7
A7	1	1	102.5	83.8
A8	1	10	106.4	87.2
A9	10	5.5	113.6	97.2

shown through interaction, perturbations, and predicted vs. actual diagnostic charts. In addition, the relationship between dependent and independent variables was established using mathematical relationships to obtain the statistical package. Finally, numerical and graphical optimization approaches determined the optimal conditions for AHAgNPs biosynthesis.

### **Entrapment efficiency**

The entrapment efficiency of nanoparticles was quantified by measuring the amount of free  $\text{AgNO}_3$  remaining in the supernatant after centrifugation at 5 000 r/min for 25 min [47]. The  $\text{AgNO}_3$  remaining in the supernatant was determined via an UV spectrophotometer (JASCO 1800) measuring absorption at 440 nm. Three replicates for nanoparticles were measured, and the entrapment efficiency (EE) was calculated as follows

$$EE = \frac{m_{\text{total AgNO}_3} - m_{\text{free AgNO}_3}}{m_{\text{total AgNO}_3}} \times 100\% \quad (1)$$

where  $m_{\text{total AgNO}_3}$  is the total mass of  $\text{AgNO}_3$  used to prepare nanoparticles and  $m_{\text{free AgNO}_3}$  is the mass of free  $\text{AgNO}_3$  remaining in the supernatant after centrifugation.

### **Synthesis and characterization of the optimized AgNPs**

The AgNPs were synthesized at optimum conditions and characterized using a UV–Vis double-beam spectrophotometer (JASCO 1800, Japan) with 1 cm paired quartz cells. The size and shape of the synthesized nanoparticles were determined by XRD (Bruker D2 Phaser X-Diffractometer), SEM (model JSM-6360), and TEM (HT7800 Ruli, Japan). The crude extract and AHAgNPs were studied for spectrometric analysis. The spectra were recorded in a wavenumber frequency ranging from 4 000 to 600  $\text{cm}^{-1}$  with a rate of 25 scans per spectrum using FT-IR (BRUKER ALPHA I, Germany). All measurements were recorded at room temperature in percent transmittance mode.

### **Determination of total phenolic and flavonoid content**

To determine the total phenolic components, the Ciocalteu method [48] was used with slight modification. First, 10 mg of AHL crude extract and AHAgNPs were separately dissolved in 10 mL of methanol. Next, 200  $\mu\text{L}$  of AHL extract and

AHAgNPs sample were taken into three test tubes, and 1.5 mL of 10% Folin–Ciocalteu reagent was added to each tube. All tubes were set aside in a dark place for 5–10 min. Finally, 1.5 mL of 5% Na<sub>2</sub>CO<sub>3</sub> was added to these solutions and mixed well by shaking. Again, all tubes were kept in the dark chamber for 2–3 h. The absorbances of all solutions were measured using a UV spectrophotometer at a constant wavelength of 750 nm. The phenolic content was measured using a gallic acid calibration curve ( $R^2 = 0.998$ ) and expressed as gallic acid equivalents. Gallic acid was used as a standard and in triplicate. Again, the absorbance was measured, and the concentration of phenolics was read (mg/mL) from the calibration line.

#### Determination of total flavonoids by a colorimetric method

The total flavonoid content of the AHL extract and AHAgNPs was estimated by a colorimetric method with aluminum chloride, as described by Ref. [48]. First, 0.25 mg of AHL extract and AHAgNPs were put into three test tubes, and 1.25 mL of water and 0.75  $\mu$ L of 5% sodium nitrate solution were added and then mixed. All tubes were left in a dark place for 10–15 min. Then, 0.15  $\mu$ L of 10% aluminum chloride solution was added to the tube, and the tubes were left in a dark place for 5–10 min to complete the reaction. Finally, 0.5 mL of 5% NaOH and 0.275 mL of deionized water were added to the tubes. Absorbances were measured for all samples at a fixed wavelength at 510 nm using a UV–Vis spectrophotometer (JASCO 1800). Quercetin was used as a standard for the calibration curve. The total content of flavonoids in AHL extract and AHAgNPs was estimated in triplicate and the results were averaged. Total flavonoids were calculated as

$$X = \frac{Am_0}{A_0m} \quad (2)$$

where  $X$  is the flavonoid content (mg/g AHL extract),  $A$  is the absorption of plant crude extract solution or AHAgNPs,  $A_0$  is the absorption of standard quercetin solution,  $m$  is the mass of crude drug extract or AHAgNPs (mg), and  $m_0$  is the mass of quercetin in the solution (mg).

#### Antioxidant assay

The antioxidant activity of AHAgNPs and the AHL extract was determined using the DPPH assay as described.

#### DPPH spectrophotometric assay

The scavenging capacity of natural plant antioxidants and nanoparticles against the stable DPPH free radicals was measured by Chavan et al. [44] and Mensor et al. [49]. Mathur et al. [50] and Irshad [51] slightly modified. AHL extract and AHAgNPs solutions (20  $\mu$ L) were added into 0.5 mL of methanolic DPPH solution and 0.48 mL of methanol in separate tubes. The mixtures were allowed to react at room temperature for 25–30 min. Methanol was used as blank, and DPPH in methanol without AHL extract and AHAgNPs was served as a positive control. After 30 min of incubation, the discoloration of the purple color was measured at 518 nm in a UV–Vis spectrophotometer. The radical scavenging activity was calculated as follows:

$$\text{Scavenging activity} = \frac{A_{518(\text{control})} - A_{518(\text{sample})}}{A_{518(\text{control})}} \times 100\% \quad (3)$$

#### Antimicrobial assay

The agar well disk diffusion method was used to check the antimicrobial ability of AHL extract and synthesized AHAgNPs.

#### Antibacterial assay

To study the antibacterial activity, four pathogenic bacterial strains, i.e., two Gram-positive (*S. aureus* ATCC 6538 and *B. subtilis* ATCC 6051) and one Gram-negative (*E. coli* ATCC 8739), were used. The antibacterial potential was determined using the disk diffusion method as described in Refs. [52, 53]. Bacterial cultures were subcultured in nutrient broth for 24 h at 35 °C. The bacterial culture was plated on nutrient media, and the desired number of holes were cut using a sterile corkscrew, ensuring proper distribution of the holes at the periphery. An 8 mm hole was used to cut holes in the nutrient agar plates. All equipment used in this test was sterilized in an autoclave, and the experiment was conducted under aseptic conditions. Cefixime-USP was used as the standard drug. Then, 100  $\mu$ g/mL samples were loaded per well as standard, control, AHL extract, and AHAgNPs, and then incubated for 24 h at 35 °C for antibacterial activity. The diameter of the inhibition zones was measured using a scale in mm.

#### Antifungal activity

Shaboraud's slant agar was prepared using agar (500 mg), peptone (250 mg), and glucose (500 mg), which were dissolved in 50 mL of distilled water, boiled, and then poured into a test tube, and the test tubes

were plugged with cotton and then sterilized in an autoclave at a pressure of 103.4 kPa (121 °C) for 15 min. After sterilization, the tubes containing Saboraud's agar were inclined to 1/2 h. Then, a pure culture of test fungi, i.e., *A. Niger*, was plated on the solid surface of these slants under aseptic conditions and then incubated at 37 °C for 24 h. The plating medium was then allowed to solidify at room temperature. Next, a sterile and non-toxic cotton swab was dipped into the standardized inoculum (turbidity adjusted to achieve contiguous growth on the petri dish). The swab was then swabbed three times over the whole agar surface of the dish, rotating the plate at a 60° angle between streaks. The applied inoculum was then allowed to dry for 10–15 min with the lid on. After that, a hole was punched into the prepared plates using a sterile well (8 mm). Next, a dose of 100 µL of AHL extract, synthesized AHAgNPs solutions, and standard drug fluconazole were applied to the hole, respectively, under aseptic conditions using a sterile micropipette. Plates were kept at room temperature for 25–30 min and then incubated at 37 °C for 24 h. The diameter of the inhibition zones was measured using a scale in mm.

## Results

### Green synthesis and confirmation of AHAgNPs

During the last two decades, traditional medicines have become a topic of interest. Thus, numerous plant extracts are being employed for the synthesis of silver nanoparticles using a biological reduction approach [54–66]. Our proposed study on the green synthesis of AHAgNPs by methanolic extract of AHL follows that trend. The color of the solutions changed from light green to darker green on increasing crude extract concentration in the absence of silver nitrate solution. In the presence of silver nitrate solution, with the increase of extract concentration, the crude extract color changed from greenish to brown and further to deep brown because of the excitation of surface plasmon vibration, indicating the formation of the silver nanoparticles. The phytochemicals present in the extract could have reduced the silver ions. The synthesized AHAgNPs were examined and confirmed using UV–Vis spectral analysis.

### Optimization and evaluation of dependent variables

The significance of the most influential factors or parameters on particle size, along with percentage

entrapment efficiency and their optimization, was assessed by full factorial design. A full factorial design is a modest-efficient design style that allows for the estimation of main effects and interactions. The advantages of using response surface morphology (RSM) for the optimization process are that it decreases time and cost, minimizes the number of experimental trials, and gives more precise outcomes [67–73]. The systematic optimization of AgNPs has been reported with plant extracts of *Azadirachta indica* [45], *Prosopis juliflora* [67], and purple heart plants [71]. Similarly, we have searched preferred conditions for AHAgNPs synthesis. The pivotal role played by the two essential factors on responses particle size with EE was statistically evaluated by full factorial design. The statistical process optimization of AgNP production using RSM was used to identify the most prominent interaction between significant parameters to produce the smallest-sized AgNPs with the greatest stability.

### ANOVA analysis report

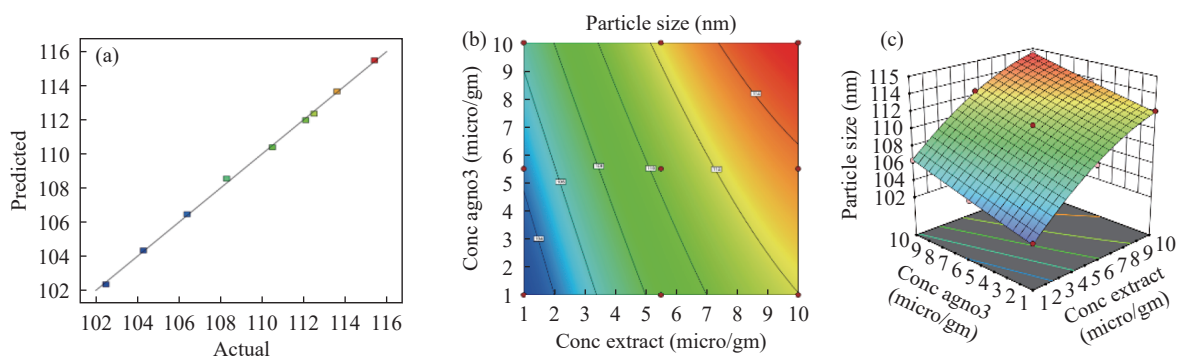
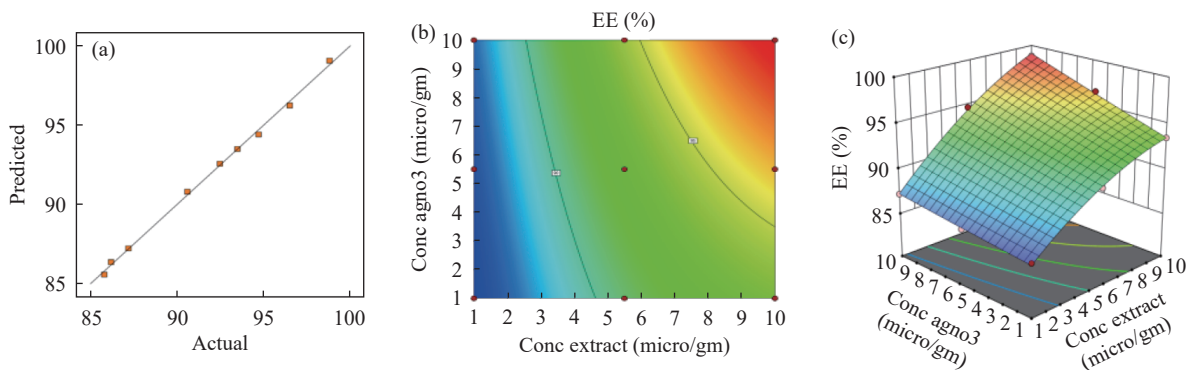
The significance and suitability of the model were evaluated using an ANOVA. Table 2 contains statistical information such as standard error, a sum of squares, *F* ratio, and *P*-value. As shown in Table 2, a *P*-value of the independent variables and their interaction in ANOVA indicates that the corresponding factors significantly affected particle size and entrapment efficiency. Three-dimensional (3D) reaction surface plots showed a variety of representations in each reaction as the two components are changed from a lower to a higher amount. This analysis provides a 3D bend of the adjustment at various component levels. It also provides a range of outline focuses based on the expected response esteem. Figures 1 and 2 show the two-dimensional (2D) & 3D response surface plots and corresponding contour plots for particle size and entrapment efficiency.

### An optimized batch of AHAgNPs

The optimized batch was selected by numerical optimization with a desirability function value closer to one. The optimum conditions of synthesizing AHAgNPs came out to be a concentration of AgNO<sub>3</sub> of 8.5 µg/mL and a concentration of AHL extract of 2.5 µg/mL. It also indicated a predicted response for synthesized AHAgNPs having particle size 108.011 nm and an entrapment efficiency of 89.45%. Furthermore, the validation studies were performed

**Table 2** Summary of variance analysis results (ANOVA)

Source	Particle size					Entrapment efficiency				
	DF	SS	MS	F	P	DF	SS	MS	F	P
Model	5	155.32	31.06	630.63	< 0.0001	5	172.22	34.44	293.14	0.0003
A	1	129.74	129.74	2633.72	< 0.0001	1	145.73	145.73	1240.31	< 0.0001
B	1	21.66	21.66	439.71	0.0002	1	19.48	19.48	165.76	0.0010
AB	1	0.0900	0.0900	1.83	0.2694	1	3.82	3.82	32.53	0.0107
A2	1	3.83	3.83	77.70	0.0031	1	3.18	3.18	27.10	0.0138
B2	1	0.0089	0.0089	0.1805	0.6996	1	0.0029	0.0029	0.0250	0.8844
Residual	3	0.1478	0.0493			3	0.3525	0.1175		
Cor total	8	155.47				8	172.57			

**Fig. 1** (a) predicted vs. actual plot, (b) 2D counter, and (c) 3D response surface plots of the selected model for particle size.**Fig. 2** (a) Predicted vs. actual plot, (b) 2D counter, and (c) 3D response surface plots of the selected model for entrapment efficiency.

on the optimized AgNPs, and the responses were evaluated. The observed values of responses for the synthesized AgNPs were found as a particle size of 107.40 nm and an entrapment efficiency of 88.20%. The observed values obtained were quite close to the predicted response (i.e., within prediction error  $\pm 10\%$ ) and the goodness of fit of the selected design and mathematical model.

### Characterization of AHAgNPs using FT-IR, XRD, SEM, and TEM

FT-IR was performed to identify the bond linkages and functional groups associated with the AHL

extract treated with AgNO<sub>3</sub>. The functional groups present in the AHL extract and AHAgNPs were analyzed using FT-IR spectroscopy. In the FT-IR analysis, AHL extract vibration stretches were observed at 3296.70, 2921.31, 2855.12, 1735.06, 1043.51, 860.73, 704.24, and 660.66 cm<sup>-1</sup>, whereas AHAgNPs peaks were found at 3266.82, 2975.62, 2896.56, 1648.84, 1450.21, 1085.73, 1043.30, and 879.38 cm<sup>-1</sup> (Fig. 3). The banding pattern of the functional group and the fingerprint region were similar to those of polyphenols specified by Chen and Mu [74] and Chavan et al. [44]. The bands at 3266.82 and 3296.70 cm<sup>-1</sup>, corresponding to O—H stretching

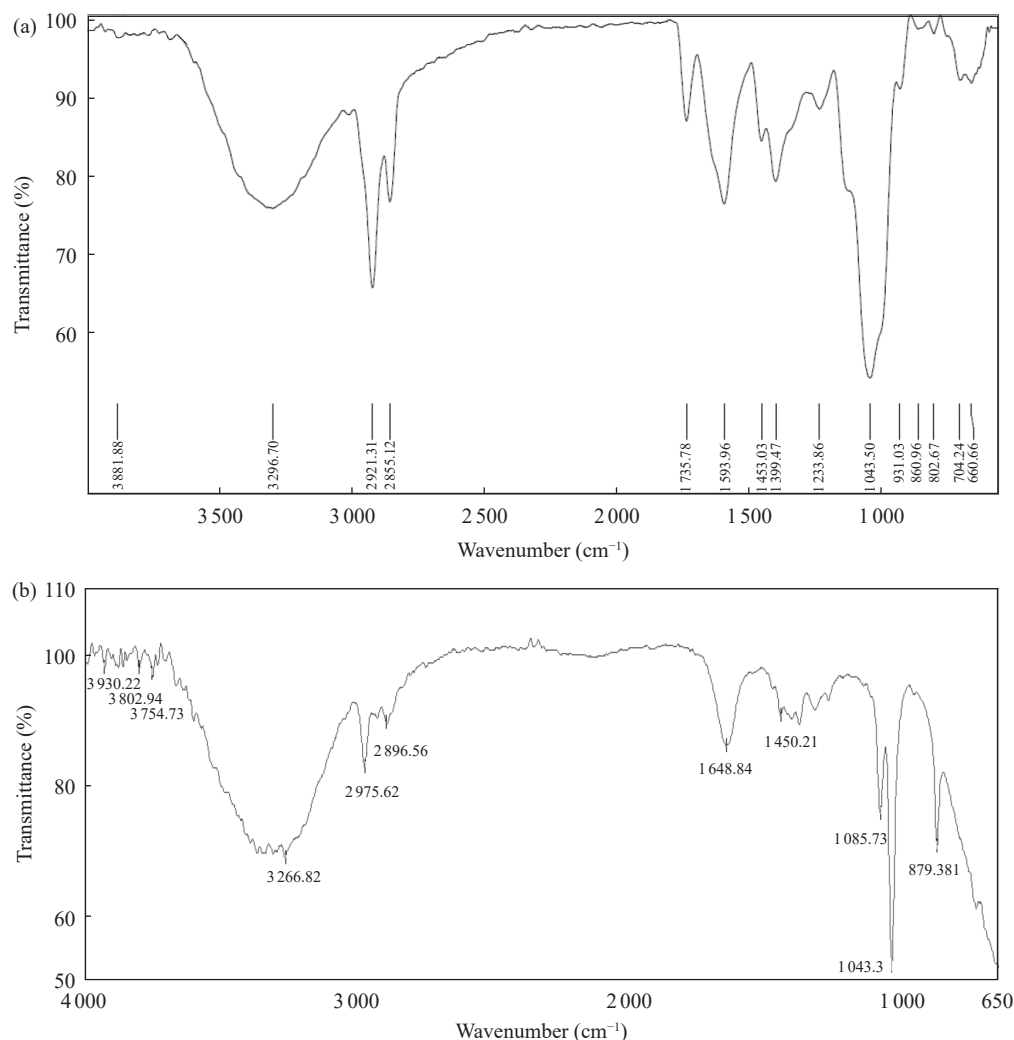


**Fig. 3** FT-IR spectra of (a) AHL extract and (b) AHAgNPs.

vibrations of the phenol group, were observed for AHAgNPs. Furthermore, 2896.56 and 2921.31  $\text{cm}^{-1}$  correspond to the C–H stretching of the aromatic compound observed for AHAgNPs. The vibration stretch at 1648.84 and 1735.06  $\text{cm}^{-1}$  is due to the C–C stretch in the aromatic ring, which confirms the presence of an aromatic group for AHAgNPs. The peak at 1511.92  $\text{cm}^{-1}$  corresponding to poly phenol's O–H bond was not found in AHL and AHAgNPs. The C–O stretching vibrations of the IR spectrum were observed at 1085.73 and 1043.351  $\text{cm}^{-1}$  in both. Based on the FT-IR investigation, it can be assumed that phenolic and flavonoid compounds present in the AHAgNPs may be involved in capping and stabilizing the nanoparticles [75].

It was found that the synthesized AHAgNPs are spherical when observed under SEM (Fig. 4). The nanoparticles' average particle size was 100–110 nm (Fig. 5). The XRD pattern of AHAgNPs (Fig. 6) suggests that the particles were crystalline. In addition, the intense diffraction peaks due to

AHAgNPs were observed. All the peaks obtained matched well with the Joint Committee on Powder Diffraction Standards file No. 04-0783 of silver [76].

### **Total phenolic, flavonoids content, and antioxidant activity of AHAgNPs and AHL extract**

The total phenolic content in the synthesized AHAgNPs was  $(18.56 \pm 1.09)$  mg of GAE/mg compared to AHL extract  $(155.76 \pm 1.12)$  mg of GAE/mg phenol content (Fig. 7). In addition, AHAgNPs were evaluated for bound flavonoid content. In our study,  $(14.40 \pm 0.03)$  mg of QE/mg  $(6.65 \pm 0.008)$  and  $(2.96 \pm 0.007)$  mg of QE/mg flavonoid content was observed in the AHL extract and AHAgNPs, respectively (Fig. 8). All the results are shown in Table 3.

### **DPPH spectrophotometric assay**

The DPPH activity results (Table 4 and Fig. 9) showed an effective free radical scavenging potential

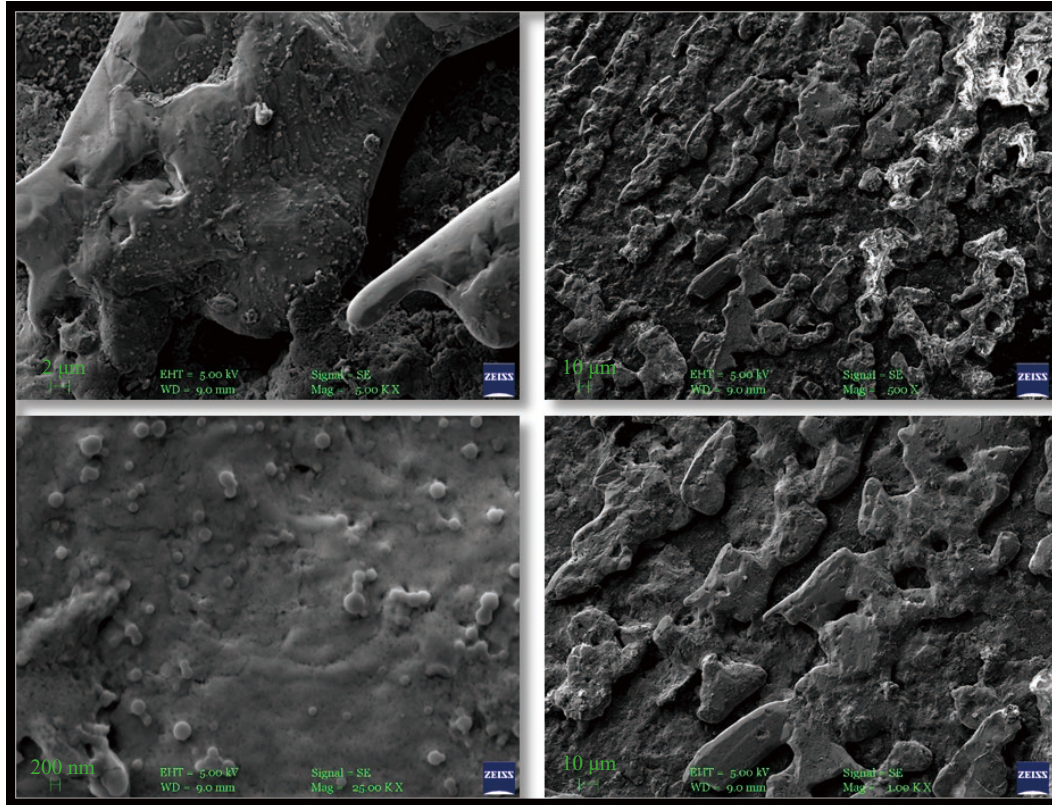


**Fig. 4** FESEM images of AHAgNPs.

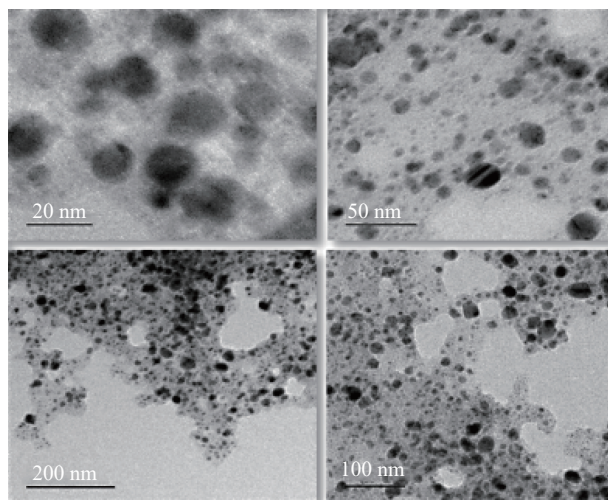


**Fig. 5** TEM images of synthesized AHAgNPs.

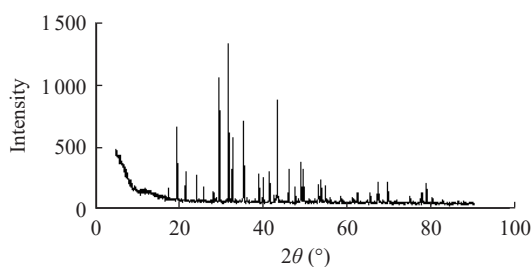


**Fig. 6** XRD pattern of synthesized AHAgNPs.

of AHAgNPs and AHL extract. The concentration-response curve of the DPPH radical scavenging

activity of the AHL methanolic extract and AHAgNPs compared with ascorbic acid is highlighted in Fig. 9. It was observed that AHAgNPs had higher activity than the AHL extract. At a concentration of 50  $\mu\text{g/mL}$ , the scavenging activity of AHAgNPs was observed to be  $91.12\% \pm 1.24\%$ . However, the DPPH radical scavenging abilities of the extracts were less than those of the standard ascorbic acid ( $98.74\% \pm 0.24\%$ ). The study showed that the AHAgNPs have proton-donating ability and could serve as free radical inhibitors or scavengers, acting possibly as primary antioxidants.

#### Antimicrobial screening of optimized AHAgNPs

Antimicrobial activity was determined by measuring the diameter of the recorded zone of inhibition. The results obtained when evaluating the antibacterial activity of control, standard, AHL, and AHAgNPs against selected pathogens are shown in Table 4 and Fig. 10. AHAgNPs and AHL showed a superior zone of inhibition compared to the control. However, AHAgNPs showed maximum activity against the selected strains due to a reduction in AHL size compared to others. AHAgNPs showed almost the same activity as cefixime against selected pathogens. The results were found to be statistically significant.

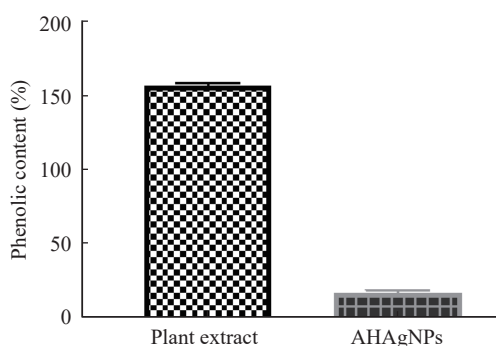


**Fig. 7** Total phenolic content ( $\mu\text{g/mL GAE/mg}$ ) determination in AHAgNPs, gold nanoparticles (AHAuNPs), and AHL extract.

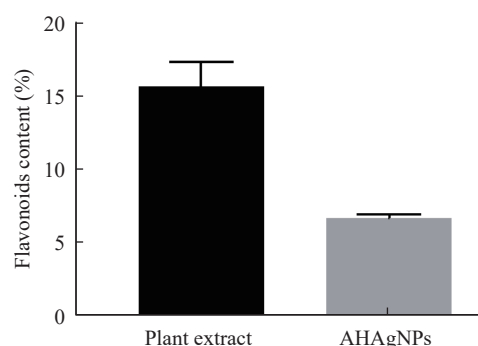


**Fig. 8** Flavonoids content ( $\mu\text{g QE/mg}$ ) determination in AHAgNPs and AHL extract.

**Table 3** Total phenolic and flavonoids content of AHAgNPs and *A. heterophyllus* leaf extract

Serial No.	Material	Phenolic content (%)	Flavonoid content (%)
1	Plant extract	155.76 ± 1.12	14.40 ± 0.03
2	AHAgNPs	18.56 ± 1.09	6.65 ± 0.008

**Table 4** DPPH radical scavenging activity of AHAgNPs and AHL extract

Concentrations ( $\mu\text{g/mL}$ )	Standard inhibition (%)	Plant extract inhibition (%)	AHAgNPs inhibition (%)
10	89.58 ± 0.78	36.28 ± 1.03	63.04 ± 1.24
20	92.43 ± 0.98	41.05 ± 0.57	77.26 ± 0.57
30	95.74 ± 1.17	44.22 ± 0.57	80.76 ± 1.00
40	98.14 ± 0.10	52.06 ± 0.08	85.26 ± 0.37
50	98.74 ± 0.24	58.22 ± 1.52	91.12 ± 1.24

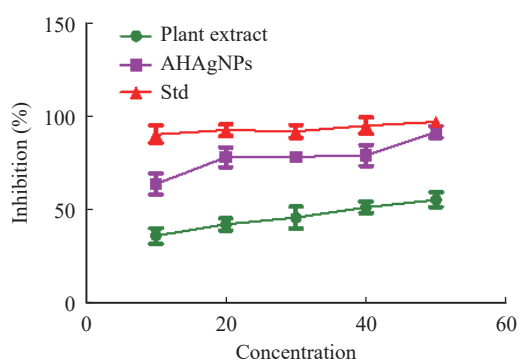


**Fig. 9** DPPH radical scavenging activity of AHAgNPs and AHL extract.

The antifungal activity of AHAgNPs and AHL extract against *A. niger*, as a fungal model, was investigated. AHAgNPs displayed an antifungal activity comparable to that of antifungal drugs such as fluconazole, as shown in Table 5 and Fig. 10 (the results were found to be statistically significant). However, AHAgNPs showed maximum activity against selected *A. niger* strains because of the reduction in AHL size compared to others. AHAgNPs showed almost the same activity as fluconazole against selected pathogens.

## Discussion

According to numerous studies, the human immune system is significantly impacted by oxidative damage. Numerous autoimmune human diseases, such as cardiac heart failure shock and atherosclerosis, are influenced by free radical processes, which play a significant pathophysiological role in these diseases. Therefore, stopping this oxidative stress and bolstering the body's immunity are essential. Numerous disorders brought on by oxidative stress are treated with an adjuvant regimen that frequently includes immunomodulatory drugs. Modern medications that treat immunosenescence and oxidative stress are pricy and have harmful side effects. Thus, using natural antioxidants to treat oxidative stress and immunosenescence is a safer option [77]. *In vitro*, antioxidant activity assessment techniques are frequently employed in ethnopharmacology research to evaluate the antioxidant potential of plants or their phytochemicals and occasionally the likely mode of action of plant antioxidants is investigated. Methods based on

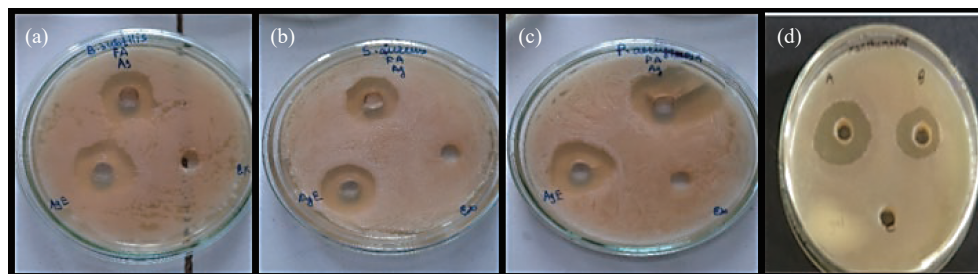


**Fig. 10** Antimicrobial activity of synthesized AHAgNPs and AHL extract against (a) *B. subtilis*, (b) *S. aureus*, (c) *E. coli*, and (d) *A. Niger*. Ag = standard, AgE = AHAgNPs, and Ex = AHL extract.

**Table 5** Antibacterial activity of AHAgNPs and AHL extract values (mean  $\pm$  SEM) are average of three experiments ( $n = 1 \times 3$ )

Bacterial strains	Inhibition zone (mm)		
	Plant extract (AHL)	AHAgNPs	STD (cefixime)
Antimicrobial activity			
<i>E. Coli</i>	13.3 $\pm$ 0.57	16.59 $\pm$ 0.52	18.8 $\pm$ 0.34
<i>B. Substalis</i>	18.33 $\pm$ 1.54	19.83 $\pm$ 0.28	20.86 $\pm$ 0.23
<i>S. Aureus</i>	15.33 $\pm$ 0.57	16.23 $\pm$ 0.40	19.92 $\pm$ 0.12
Antifungal activity			
Bacterial strains	Plant extract (AHL)	AHAgNPs	STD (fluconazole)
<i>A. Niger</i>	13.76 $\pm$ 0.57	14.20 $\pm$ 0.64	20.6 $\pm$ 1.03

hydrogen atom transfer (HAT) and electron transfer can be used to evaluate the antioxidants. While single electron transfer (SET)-based methods assess an antioxidant's capacity to transfer one electron to reduce any chemical, including metals, carbonyls, and free radicals, HAT-based methods assess an antioxidant's capacity to scavenge free radicals through hydrogen donation that generates stable compounds [78].

The AHL extract had a much greater total flavonoid and phenol concentration than AHAgNPs. Therefore, it can be considered that these extracts contain the primary polyphenolic components. The AHL extract demonstrated the highest lowering capacity through efficient silver ion chelation. Because of the presence of phenolics in this extract, it was also discovered to be the most efficient in all *in vitro* experiments. According to a literature reviews by Devi et al., Omar et al., and Thapa et al. [32, 79, 80], AHL extract demonstrated excellent antioxidant activity. Additionally, the results demonstrated that the plant extract alone was responsible for the majority of the antioxidant activity and that AHAgNPs did not significantly contribute to the antioxidant activity, as seen by the increase in antioxidant activity of AHAgNPs compared to AHL extract. The antioxidant capacity may increase

significantly due to the chelation with metal ions, as per the findings of Ajisaka and coworkers [81]. Moreover, AHAgNPs had higher antioxidant properties, which may lead to more silver ion reduction than the extract [82]. Thus, NPs are considered an alternative to antibiotics since they can occasionally effectively circumvent bacteria drug resistance [83–86].

Uncontrolled antibiotic usage has given rise to several public health problems, including the advent of superbugs resistant to all known antibiotics and epidemics untreatable by medicine [87]. Drug resistance is a critical issue that requires the development of new and powerful bactericidal materials, and NPs have been proposed as a viable solution to this issue [88–93]. The metal, metal oxide, and organic nanoparticle antimicrobial nanomaterials currently in use have a variety of intrinsic and modified chemical characteristics. Additionally, the surface area in the nano state increased, increasing the contact area between  $\text{Ag}^0$  and the microbe [94]. To test the antibacterial activity, we made nanoparticles from the leaf extract of *A. heterophyllus*.

No literature was found on the synthesis of AgNPs from AHLs. In this study, the antibacterial activity of AHAgNPs was investigated against *S. aureus*, *B.*

*subtilis*, and *E. coli* as model bacteria and the model for antifungal activity against *A. Niger*. AHAgNPs showed a strong antibacterial and antifungal activity against the tested strains of bacteria and fungi.

## Conclusion

We synthesized AHAgNPs from *A. heterophyllus* leaf extract by biological synthesis technique using factorial design, which is simple and environmentally friendly. AHAgNPs with an average particle size of 100–110 nm were obtained. They are easy, cost effective, and free of harmful and toxic chemicals. We observed total phenolic and flavonoid content in AHAgNPs and AHL extract. Total phenolic and total flavonoid content correlated significantly with total antioxidant activity and free radical scavenging capacity. AHAgNPs showed a strong antibacterial and antifungal activity against the tested bacterial and fungal strains. This may be due to the presence of silver ions in AHAgNPs.

## CRedit Author Statement

**R.R. Chavan:** Conceptualization, methodology, software, writing, and original draft preparation. **M.A. Bhutkar:** Visualization, investigation, software supervision, writing, reviewing and editing. **S.D. Bhinge:** Conceptualization, writing- reviewing, and editing.

## Acknowledgment

The authors are thankful to Dr. S. A. Mohite, Principal, Rajarambapu College of Pharmacy, Kasegaon (Maharashtra) for providing the necessary facilities to carry out the research work.

## Conflict of Interest

The authors declare that they have no conflict of interest to disclose.

## Supporting Information

Supporting information to this article can be found online at <http://doi.org/10.26599/NBE.2023.9290011>.

## References

- [1] D. Blondeau, L. Roy, S. Dumont, et al. Physicians' and pharmacists' attitudes toward the use of sedation at the end of life: Influence of prognosis and type of suffering. *Journal of Palliative Care*, 2005, 21(4): 238–245. <https://doi.org/10.1177/082585970502100402>
- [2] L. Zhang, F.X. Gu, J.M. Chan, et al. Nanoparticles in medicine: Therapeutic applications and developments. *Clinical Pharmacology and Therapeutics*, 2008, 83(5): 761–769. <https://doi.org/10.1038/sj.clpt.6100400>
- [3] S. Kundu, V. Maheshwari, S.J. Niu, et al. Polyelectrolyte mediated scalable synthesis of highly stable silver nanocubes in less than a minute using microwave irradiation. *Nanotechnology*, 2008, 19(6): 065604. <https://doi.org/10.1088/0957-4484/19/6/065604>
- [4] K. Okitsu, Y. Mizukoshi, T.A. Yamamoto, et al. Sonochemical synthesis of gold nanoparticles on chitosan. *Materials Letters*, 2007, 61(16): 3429–3431. <https://doi.org/10.1016/j.matlet.2006.11.090>
- [5] P.P. Gan, S.H. Ng, Y. Huang, et al. Green synthesis of gold nanoparticles using palm oil mill effluent (POME): A low-cost and eco-friendly viable approach. *Bioresource Technology*, 2012, 113: 132–135. <https://doi.org/10.1016/j.biortech.2012.01.015>
- [6] K.B. Narayanan, N. Sakthivel. Biological synthesis of metal nanoparticles by microbes. *Advances in Colloid and Interface Science*, 2010, 156(1–2): 1–13. <https://doi.org/10.1016/j.cis.2010.02.001>
- [7] S. Narayanan, B.N. Sathy, U. Mony, et al. Biocompatible magnetite/gold nanohybrid contrast agents via green chemistry for MRI and CT bioimaging. *ACS Applied Materials & Interfaces*, 2012, 4(1): 251–260. <https://doi.org/10.1021/am201311c>
- [8] Sharma, H. S., Ali, S. F., Hussain, S. M., Schlager, J. J., Sharma, A. Influence of engineered nanoparticles from metals on the blood-brain barrier permeability, cerebral blood flow, brain edema and neurotoxicity. An experimental study in the rat and mice using biochemical and morphological approaches. *Journal of Nanoscience and Nanotechnology*, 2009, 9(8): 5055–5072. <https://doi.org/10.1166/jnn.2009.GR09>
- [9] L. Castro, M.L. Blázquez, J.A. Muñoz, et al. Biological synthesis of metallic nanoparticles using algae. *IET Nanobiotechnology*, 2013, 7(3): 109–116. <https://doi.org/10.1049/iet-nbt.2012.0041>
- [10] B.A. Zsembik. Health issues in Latino families and households. In: Handbook of families and health: interdisciplinary perspectives. SAGE Publications, 2006: 40–61. <https://doi.org/10.4135/9781452231631.n3>
- [11] S. Poulouse, T. Panda, P.P. Nair, et al. Biosynthesis of silver nanoparticles. *Journal of Nanoscience and Nanotechnology*, 2014, 14(2): 2038–2049. <https://doi.org/10.1166/jnn.2014.9019>
- [12] K. Vithiya, S. Sen. Biosynthesis of nanoparticles. *International Journal of Pharmaceutical Science and Research*, 2011, 2(11): 2781–2785.
- [13] S. Sunkar, C.V. Nachiyar. Biogenesis of antibacterial silver nanoparticles using the endophytic bacterium *Bacillus cereus* isolated from *Garcinia xanthochymus*. *Asian Pacific Journal of Tropical Biomedicine*, 2012, 2(12): 953–959. [https://doi.org/10.1016/S2221-1691\(13\)60006-4](https://doi.org/10.1016/S2221-1691(13)60006-4)
- [14] N. Madubuonu, S.O. Aisida, I. Ahmad, et al. Bio-inspired iron oxide nanoparticles using *Psidium guajava* aqueous extract for antibacterial activity. *Applied Physics A: Materials Science and Processing*, 2020, 126(1): 1–8. <https://doi.org/10.1007/s00339-019-3249-6>

- [15] S. Das, A. Das, A. Maji, et al. A compact study on impact of multiplicative *Streblus asper* inspired biogenic silver nanoparticles as effective photocatalyst, good antibacterial agent and interplay upon interaction with human serum albumin. *Journal of Molecular Liquids*, 2018, 259: 18–29. <https://doi.org/10.1016/j.molliq.2018.02.111>
- [16] E.C. Njagi, H. Huang, L. Stafford, et al. Biosynthesis of iron and silver nanoparticles at room temperature using aqueous sorghum bran extracts. *Langmuir: the ACS Journal of Surfaces and Colloids*, 2011, 27(1): 264–271. <https://doi.org/10.1021/la103190n>
- [17] R. Joseph, A. Naugolny, M. Feldman, et al. Cationic pillararenes potently inhibit biofilm formation without affecting bacterial growth and viability. *Journal of the American Chemical Society*, 2016, 138(3): 754–757. <https://doi.org/10.1021/jacs.5b11834>
- [18] H. C. Flemming, J. Wingender, U. Szewzyk, et al. Biofilms: An emergent form of bacterial life. *Nature Reviews Microbiology*, 2016, 14(9): 563–575. <https://doi.org/10.1038/nrmicro.2016.94>
- [19] J.H. Wu, F.Y. Li, X. Hu, et al. Responsive assembly of silver nanoclusters with a biofilm locally amplified bactericidal effect to enhance treatments against multi-drug-resistant bacterial infections. *ACS Central Science*, 2019, 5(8): 1366–1376. <https://doi.org/10.1021/acscentsci.9b00359>
- [20] A.K. Gupta, M.A. Rather, A. Kumar Jha, et al. *Artocarpus lakoocha* roxb. and *artocarpus heterophyllus* lam. flowers: New sources of bioactive compounds. *Plants*, 2020, 9(10): 1329. <https://doi.org/10.3390/plants9101329>
- [21] K.E. Jones, N.G. Patel, M.A. Levy, et al. Global trends in emerging infectious diseases. *Nature*, 2008, 451(7181): 990–993. <https://doi.org/10.1038/nature06536>
- [22] S.L. Jagadeesh, B.S. Reddy, G.S.K. Swamy, et al. Chemical composition of jackfruit (*Artocarpus heterophyllus* Lam.) selections of Western Ghats of India. *Food Chemistry*, 2007, 102(1): 361–365. <https://doi.org/10.1016/j.foodchem.2006.05.027>
- [23] R.A.S.N. Ranasinghe, S.D.T. Maduwanthi, R.A.U.J. Marapana. Nutritional and health benefits of jackfruit (*Artocarpus heterophyllus* Lam.): A review. *International Journal of Food Science*, 2019, 2019: 4327183. <https://doi.org/10.1155/2019/4327183>
- [24] R. Srivastava, A. Singh. Jackfruit (*Artocarpus heterophyllus* Lam) Biggest Fruit with High Nutritional and Pharmacological Values: A Review. *International Journal of Current Microbiology and Applied Sciences*, 2020, 9(8): 764–774. <https://doi.org/10.20546/ijcmas.2020.908.082>
- [25] F. Chahud, L.N.Z. Ramalho, F.S. Ramalho, et al. The lectin KM+ induces corneal epithelial wound healing in rabbits. *International Journal of Experimental Pathology*, 2009, 90(2): 166–173. <https://doi.org/10.1111/j.1365-2613.2008.00626.x>
- [26] S.C. Fang, C.L. Hsu, G.C. Yen. Anti-inflammatory effects of phenolic compounds isolated from the fruits of *Artocarpus heterophyllus*. *Journal of Agricultural and Food Chemistry*, 2008, 56(12): 4463–4468. <https://doi.org/10.1021/jf800444g>
- [27] M.B. Trindade, J.L.S. Lopes, A. Soares-Costa, et al. Structural characterization of novel chitin-binding lectins from the genus *Artocarpus* and their antifungal activity. *Biochimica et Biophysica Acta - Proteins and Proteomics*, 2006, 1764(1): 146–152. <https://doi.org/10.1016/j.bbapap.2005.09.011>
- [28] M.R. Fernando, N. Wickramasinghe, M.I. Thabrew, et al. Effect of *Artocarpus heterophyllus* and *Asteracanthus longifolia* on glucose tolerance in normal human subjects and in maturity-onset diabetic patients. *Journal of Ethnopharmacology*, 1991, 31(3): 277–282. [https://doi.org/10.1016/0378-8741\(91\)90012-3](https://doi.org/10.1016/0378-8741(91)90012-3)
- [29] A. Eve, A.A. Aliero, D. Nalubiri, et al. *In vitro* antibacterial activity of crude extracts of *artocarpus heterophyllus* seeds against selected diarrhoea-causing superbug bacteria. *The Scientific World Journal*, 2020, 2020: 9813970. <https://doi.org/10.1155/2020/9813970>
- [30] A. Agarwal, A. Kumar, B.K. Singh, et al. A review on extraction and phytochemical screening methods. *Research in Pharmacy and Health Sciences*, 2016, 2(2): 130–137. <https://doi.org/10.32463/rphs.2016.v02i02.25>
- [31] F.N. Ko, Z.J. Cheng, C.N. Lin, et al. Scavenger and antioxidant properties of prenylflavones isolated from *Artocarpus heterophyllus*. *Free Radical Biology & Medicine*, 1998, 25(2): 160–168. [https://doi.org/10.1016/S0891-5849\(98\)00031-8](https://doi.org/10.1016/S0891-5849(98)00031-8)
- [32] P.S. Sreeja Devi, N.S. Kumar, K.K. Sabu. Phytochemical profiling and antioxidant activities of different parts of *Artocarpus heterophyllus* Lam. (Moraceae): A review on current status of knowledge. *Future Journal of Pharmaceutical Sciences*, 2021, 7: 30. <https://doi.org/10.1186/s43094-021-00178-7>
- [33] A.K. Nayak, M.S. Hasnain, J. Malakar. Development and optimization of hydroxyapatite-ofloxacin implants for possible bone delivery in osteomyelitis treatment. *Current Drug Delivery*, 2013, 10(2): 241–250. <https://doi.org/10.2174/1567201811310020008>
- [34] M.S. Alam, A. Garg, F.H. Pottoo, et al. Gum ghatti mediated, one pot green synthesis of optimized gold nanoparticles: Investigation of process-variables impact using Box-Behnken based statistical design. *International Journal of Biological Macromolecules*, 2017, 104(Pt A): 758–767. <https://doi.org/10.1016/j.ijbiomac.2017.05.129>
- [35] Z.Z. Ge, M.Y. Yang, Y.L. Wang, et al. Preparation and evaluation of orally disintegrating tablets of taste masked phenacylonate HCl using ion-exchange resin. *Drug Development and Industrial Pharmacy*, 2015, 41(6): 934–941. <https://doi.org/10.3109/03639045.2014.914529>
- [36] M.S. Hasnain, S.A. Ansari, S. Rao, et al. QbD-Driven Development and Validation of Liquid Chromatography Tandem Mass Spectrometric Method for the Quantitation of Sildenafil in Human Plasma. *Journal of Chromatographic Science*, 2017, 55(6): 587–594. <https://doi.org/10.1093/chromsci/bmx010>
- [37] M.S. Hasnain, S. Rao, M.K. Singh, et al. Development and validation of LC-MS/MS method for the quantitation of lenalidomide in human plasma using Box-Behnken experimental design. *The Analyst*, 2013, 138(5): 1581–1588. <https://doi.org/10.1039/c2an36701g>
- [38] M.S. Hasnain, S. Rao, M.K. Singh, et al. Development and validation of an improved LC-MS/MS method for the quantification of desloratadine and its metabolite in human plasma using deuterated desloratadine as internal standard. *Journal of Pharmacy and Bioallied Sciences*, 2013, 5(1): 74–79. <https://doi.org/10.4103/0975-7406.106571>
- [39] A.K. Nayak, S. Kalia, M.S. Hasnain. Optimization of aceclofenac-loaded pectinate-poly(vinyl pyrrolidone) beads by response surface methodology. *International Journal of Biological Macromolecules*, 2013, 62: 194–202. <https://doi.org/10.1016/j.ijbiomac.2013.08.043>
- [40] A.K. Nayak, D. Pal, J. Pradhan, et al. Fenugreek seed mucilage-alginate mucoadhesive beads of metformin HCl: Design, optimization and evaluation. *International Journal of Biological Macromolecules*, 2013, 54: 144–154. <https://doi.org/10.1016/j.ijbiomac.2012.12.008>
- [41] A.K. Nayak, D. Pal, M.S. Hasnain. Development, optimization and in vitro-in vivo evaluation of pioglitazone-loaded jackfruit seed starch-alginate beads. *Current Drug Delivery*, 2013, 10: 608–619. <https://doi.org/10.2174/1567201811310050012>

- [42] J. Malakar, K. Das, A.K. Nayak. Statistical optimization in formulation development of in situ cross-linked matrix tablets for sustained salbutamol sulfate release. *Polymer Medicine*, 2014, 44: 221–230.
- [43] N. Prabhu, D.T. Raj, K. Yamuna Gowri, et al. Synthesis of silver phyto nanoparticles and their antibacterial efficacy. *Digest Journal of Nanomaterials and Biostructures*, 2010, 5(1): 185–189.
- [44] R.R. Chavan, S.D. Bhinge, M.A. Bhutkar, et al. Characterization, antioxidant, antimicrobial and cytotoxic activities of green synthesized silver and iron nanoparticles using alcoholic Blumea eriantha DC plant extract. *Materials Today Communications*, 2020, 24: 101320. <https://doi.org/10.1016/j.mtcomm.2020.101320>
- [45] M. Singhal, A.H. Bahkali. Design, synthesis and optimization of silver nanoparticles using Azadirachta indica bark extract and its antibacterial application, 2022. Available at <https://doi.org/10.21203/rs.3.rs-1928723/v1>
- [46] Two-level fractional factorial designs. In: A modern theory of factorial designs. Springer, 2006: 49–84. [https://doi.org/10.1007/0-387-37344-6\\_3](https://doi.org/10.1007/0-387-37344-6_3)
- [47] Y. Mi, J. Zhang, L. Zhang, et al. Synthesis, characterization, and evaluation of nanoparticles loading adriamycin based on 2-hydroxypropyltrimethyl ammonium chloride chitosan grafting folic acid. *Polymers*, 2021, 13(14): 2229. <https://doi.org/10.3390/polym13142229>
- [48] M.A. Hossain, K.A. AL-Raqmi, Z.H. AL-Mijzy, et al. Study of total phenol, flavonoids contents and phytochemical screening of various leaves crude extracts of locally grown Thymus vulgaris. *Asian Pacific Journal of Tropical Biomedicine*, 2013, 3(9): 705–710. [https://doi.org/10.1016/S2221-1691\(13\)60142-2](https://doi.org/10.1016/S2221-1691(13)60142-2)
- [49] L.L. Mensor, F.S. Menezes, G.G. Leitão, et al. Screening of Brazilian plant extracts for antioxidant activity by the use of DPPH free radical method. *Phytotherapy Research*, 2001, 15(2): 127–130. <https://doi.org/10.1002/ptr.687>
- [50] R. Mathur, R. Vijayvergia. Determination of Total Flavonoid and Phenol Content in Mimosa elengi Linn. *International Journal of Pharmaceutical Sciences and Research*, 2017, 8(12): 5282–5285. [https://doi.org/10.13040/IJPSR.0975-8232.8\(12\).5282-85](https://doi.org/10.13040/IJPSR.0975-8232.8(12).5282-85)
- [51] M. Irshad. Antioxidant and antimicrobial activities of essential oil of Skimmia laureola growing wild in the State of Jammu and Kashmir. *Journal of Medicinal Plants Research*, 2012, 6(9): 1680–1684. <https://doi.org/10.5897/jmpr11.1470>
- [52] S.D. Bhinge, M.A. Bhutkar, D.S. Randive, et al. Formulation development and evaluation of antimicrobial polyherbal gel. *Annales Pharmaceutiques Francaises*, 2017, 75(5): 349–358. <https://doi.org/10.1016/j.pharma.2017.04.006>
- [53] S.S. Shankar, A. Rai, A. Ahmad, et al. Rapid synthesis of Au, Ag, and bimetallic Au core-Ag shell nanoparticles using Neem (Azadirachta indica) leaf broth. *Journal of Colloid and Interface Science*, 2004, 275(2): 496–502. <https://doi.org/10.1016/j.jcis.2004.03.003>
- [54] A.D. Dwivedi, K. Gopal. Biosynthesis of silver and gold nanoparticles using Chenopodium album leaf extract. *Colloids and Surfaces A: Physicochemical and Engineering Aspects*, 2010, 369(1–3): 27–33. <https://doi.org/10.1016/j.colsurfa.2010.07.020>
- [55] J. Hussein, M.E. El-Naggar, M.M.G. Fouda, et al. The efficiency of blackberry loaded AgNPs, AuNPs and Ag@AuNPs mediated pectin in the treatment of cisplatin-induced cardiotoxicity in experimental rats. *International Journal of Biological Macromolecules*, 2020, 159: 1084–1093. <https://doi.org/10.1016/j.ijbiomac.2020.05.115>
- [56] A.K. Jha, K. Prasad. Green synthesis of silver nanoparticles using cycas leaf. *International Journal of Green Nanotechnology: Physics and Chemistry*, 2010, 1(2): P110–P117. <https://doi.org/10.1080/19430871003684572>
- [57] M. Mourabet, A. El Rhilassi, H. El Boujaady, et al. Use of response surface methodology for optimization of fluoride adsorption in an aqueous solution by Brushite. *Arabian Journal of Chemistry*, 2017, 10: S3292–S3302. <https://doi.org/10.1016/j.arabjc.2013.12.028>
- [58] A.-R. Phull, Q. Abbas, A. Ali, et al. Antioxidant, cytotoxic and antimicrobial activities of green synthesized silver nanoparticles from crude extract of *Bergenia ciliata*. *Future Journal of Pharmaceutical Sciences*, 2016, 2(1): 31–36. <https://doi.org/10.1016/j.fjps.2016.03.001>
- [59] R.W. Rajesh, L.R. Jaya, K.S. Niranjan, et al. Phytosynthesis of silver nanoparticle using *Gliricidia sepium* (Jacq.). *Current Nanoscience*, 2009, 5(1): 117–122. <https://doi.org/10.2174/157341309787314674>
- [60] S.M. Roopan, Rohit, G. Madhumitha, et al. Low-cost and eco-friendly phyto-synthesis of silver nanoparticles using *Cocos nucifera* coir extract and its larvicidal activity. *Industrial Crops and Products*, 2013, 43(1): 631–635. <https://doi.org/10.1016/j.indcrop.2012.08.013>
- [61] K.P. Shejawal, D.S. Randive, S.D. Bhinge, et al. Green synthesis of silver and iron nanoparticles of isolated proanthocyanidin: its characterization, antioxidant, antimicrobial, and cytotoxic activities against COLO320DM and HT29. *Journal of Genetic Engineering and Biotechnology*, 2020, 18: 43. <https://doi.org/10.1186/s43141-020-00058-2>
- [62] Z.K. Taha, S.N. Hawar, G.M. Sulaiman. Extracellular biosynthesis of silver nanoparticles from *Penicillium italicum* and its antioxidant, antimicrobial and cytotoxicity activities. *Biotechnology Letters*, 2019, 41(8–9): 899–914. <https://doi.org/10.1007/s10529-019-02699-x>
- [63] R. Veerasamy, T.Z. Xin, S. Gunasagaran, et al. Biosynthesis of silver nanoparticles using mangosteen leaf extract and evaluation of their antimicrobial activities. *Journal of Saudi Chemical Society*, 2011, 15(2): 113–120. <https://doi.org/10.1016/j.jscs.2010.06.004>
- [64] Y. Yamamoto, S. Tamura, T. Kumon, et al. A case of mucocele of the appendix; diffusion weighted MRI appearance. *Japanese Journal of Clinical Radiology*, 2007, 52(10): 1265–1269.
- [65] A.K. Jha, K. Prasad, K. Prasad, et al. Plant system: Nature's nanofactory. *Colloids and Surfaces B, Biointerfaces*, 2009, 73(2): 219–223. <https://doi.org/10.1016/j.colsurfb.2009.05.018>
- [66] S.P. Dubey, M. Lahtinen, M. Sillanpää. Green synthesis and characterizations of silver and gold nanoparticles using leaf extract of *Rosa rugosa*. *Colloids and Surfaces A: Physicochemical and Engineering Aspects*, 2010, 364: 34–41. <https://doi.org/10.1016/j.colsurfa.2010.04.023>
- [67] G. Arya, R.M. Kumari, N. Gupta, et al. Green synthesis of silver nanoparticles using *Prosopis juliflora* bark extract: Reaction optimization, antimicrobial and catalytic activities. *Artificial Cells, Nanomedicine, and Biotechnology*, 2018, 46(5): 985–993. <https://doi.org/10.1080/21691401.2017.1354302>
- [68] J. Das, P. Velusamy. Biogenic synthesis of antifungal silver nanoparticles using aqueous stem extract of banana. *Nano Biomedicine and Engineering*, 2013, 5(1): 34–38. <https://doi.org/10.5101/nbe.v5i1>
- [69] M.S. Hasnain, M.N. Javed, M.S. Alam, et al. Purple heart plant leaves extract-mediated silver nanoparticle synthesis: Optimization by Box-Behnken design. *Materials Science & Engineering C, Materials for*

- Biological Applications*, 2019, 99: 1105–1114. <https://doi.org/10.1016/j.msec.2019.02.061>
- [70] M.J. Kim, J.N. Hyun, J.A. Kim, et al. Relationship between phenolic compounds, anthocyanins content and antioxidant activity in colored barley germplasm. *Journal of Agricultural and Food Chemistry*, 2007, 55(12): 4802–4809. <https://doi.org/10.1021/jf0701943>
- [71] G. Nikaeen, S. Yousefinejad, S. Rahmdel, et al. Central composite design for optimizing the biosynthesis of silver nanoparticles using plantago major extract and investigating antibacterial, antifungal and antioxidant activity. *Scientific Reports*, 2020, 10(1): 9642. <https://doi.org/10.1038/s41598-020-66357-3>
- [72] A.M. Othman, M.A. Elsayed, A.M. Elshafei, et al. Application of response surface methodology to optimize the extracellular fungal mediated nanosilver green synthesis. *Journal of Genetic Engineering and Biotechnology*, 2017, 15(2): 497–504. <https://doi.org/10.1016/j.jgeb.2017.08.003>
- [73] N. Rahman, P. Varshney. Assessment of ampicillin removal efficiency from aqueous solution by polydopamine/zirconium(iv) iodate: Optimization by response surface methodology. *RSC Advances*, 2020, 10(34): 20322–20337. <https://doi.org/10.1039/d0ra02061c>
- [74] C. Chen, S. Mu. The electrochemical preparation of polyphenol with conductivity. *Chinese Journal of Polymer Science*, 2002, 20: 309–316.
- [75] N.J. Reddy, D. Nagoor Vali, M. Rani, et al. Evaluation of antioxidant, antibacterial and cytotoxic effects of green synthesized silver nanoparticles by Piper longum fruit. *Materials Science & Engineering C, Materials for Biological Applications*, 2014, 34: 115–122. <https://doi.org/10.1016/j.msec.2013.08.039>
- [76] S.V. Kumar, S.P. Kumar, D. Rupesh, et al. Journal of Chemical and Pharmaceutical Research preparations. *Journal of Chemical and Pharmaceutical Research*, 2011, 3(1): 675–684.
- [77] D.M. Kasote, S.S. Katyare, M.V. Hegde, et al. Significance of antioxidant potential of plants and its relevance to therapeutic applications. *International Journal of Biological Sciences*, 2015, 11(8): 982–991. <https://doi.org/10.7150/ijbs.12096>
- [78] Munteanu, I.G., Apetrei, C. Analytical methods used in determining antioxidant activity: A review. *International Journal of Molecular Sciences*, 2021, 22(7): 3380. <https://doi.org/10.3390/ijms22073380>
- [79] H.S. Omar, H.A. El-Beshbishy, Z. Moussa, et al. Antioxidant activity of *Artocarpus heterophyllus* Lam. (Jack Fruit) leaf extracts: Remarkable attenuations of hyperglycemia and hyperlipidemia in streptozotocin-diabetic rats. *The Scientific World Journal*, 2011, 11: 788–800. <https://doi.org/10.1100/tsw.2011.71>
- [80] N. Thapa, P. Thapa, J. Bhandari, et al. Study of Phytochemical, Antioxidant and Antimicrobial Activity of *Artocarpus heterophyllus*. *Nepal Journal of Biotechnology*, 2016, 4(1): 47–53. <https://doi.org/10.3126/njb.v4i1.16347>
- [81] K. Ajisaka, Y. Oyanagi, T. Miyazaki, et al. Effect of the chelation of metal cation on the antioxidant activity of chondroitin sulfates. *Bioscience, Biotechnology, and Biochemistry*, 2016, 80(6): 1179–1185. <https://doi.org/10.1080/09168451.2016.1141036>
- [82] A. Saxena, R.M. Tripathi, F. Zafar, et al. Green synthesis of silver nanoparticles using aqueous solution of *Ficus benghalensis* leaf extract and characterization of their antibacterial activity. *Materials Letters*, 2012, 67: 91–94. <https://doi.org/10.1016/j.matlet.2011.09.038>
- [83] W. Gao, Y. Chen, Y. Zhang, et al. Nanoparticle-based local antimicrobial drug delivery. *Advanced Drug Delivery Reviews*, 2018, 127: 46–57. <https://doi.org/10.1016/j.addr.2017.09.015>
- [84] N.Y. Lee, W. C. Ko, P.R. Hsueh. Nanoparticles in the treatment of infections caused by multidrug-resistant organisms. *Frontiers in Pharmacology*, 2019, 10: 1153. <https://doi.org/10.3389/fphar.2019.01153>
- [85] G.R. Rudramurthy, M.K. Swamy, U.R. Sinniah, et al. Nanoparticles: Alternatives against drug-resistant pathogenic microbes. *Molecules*, 2016, 21(7): 836. <https://doi.org/10.3390/molecules21070836>
- [86] L.L. Wang, C. Hu, L.Q. Shao. The antimicrobial activity of nanoparticles: Present situation and prospects for the future. *International Journal of Nanomedicine*, 2017, 12: 1227–1249. <https://doi.org/10.2147/IJN.S121956>
- [87] B. Khameneh, R. Diab, K. Ghazvini, et al. Breakthroughs in bacterial resistance mechanisms and the potential ways to combat them. *Microbial Pathogenesis*, 2016, 95: 32–42. <https://doi.org/10.1016/j.micpath.2016.02.009>
- [88] N. Beyth, Y. Hourri-Haddad, A. Domb, et al. Alternative antimicrobial approach: Nano-antimicrobial materials. *Evidence-Based Complementary and Alternative Medicine: ECAM*, 2015, 2015: 246012. <https://doi.org/10.1155/2015/246012>
- [89] M. Mühlhling, A. Bradford, J.W. Readman, et al. An investigation into the effects of silver nanoparticles on antibiotic resistance of naturally occurring bacteria in an estuarine sediment. *Marine Environmental Research*, 2009, 68(5): 278–283. <https://doi.org/10.1016/j.marenvres.2009.07.001>
- [90] R.Y. Pelgrift, A.J. Friedman. Nanotechnology as a therapeutic tool to combat microbial resistance. *Advanced Drug Delivery Reviews*, 2013, 65(13–14): 1803–1815. <https://doi.org/10.1016/j.addr.2013.07.011>
- [91] M.A. Bhutkar, D.S. Randive, S.D. Bhinge, et al. Development of gold, silver and iron nanoparticles of isolated berberine: Its characterization, antimicrobial, and cytotoxic activities against COLO320DM and Hela cells. *Gold Bulletin*, 2022, 55(1): 93–103. <https://doi.org/10.1007/s13404-022-00309-9>
- [92] R.R. Chavan, S.D. Bhinge, M.A. Bhutkar, et al. In vivo and in vitro hair growth-promoting effect of silver and iron nanoparticles synthesized via *Blumea eriantha* DC plant extract. *Journal of Cosmetic Dermatology*, 2021, 20(4): 1283–1297. <https://doi.org/10.1111/jocd.13713>
- [93] K.P. Shejawal, D.S. Randive, S.D. Bhinge, et al. Green synthesis of silver, iron and gold nanoparticles of lycopene extracted from tomato: Their characterization and cytotoxicity against COLO320DM, HT29 and Hella cell. *Journal of Materials Science Materials in Medicine*, 2021, 32(2): 19. <https://doi.org/10.1007/s10856-021-06489-8>
- [94] S. Maiti, D. Krishnan, G. Barman, et al. Antimicrobial activities of silver nanoparticles synthesized from *Lycopersicon esculentum* extract. *Journal of Analytical Science and Technology*, 2014, 5(1): 1–7. <https://doi.org/10.1186/s40543-014-0040-3>

© The author(s) 2023. This is an open-access article distributed under the terms of the Creative Commons Attribution 4.0 International License (CC BY) (<http://creativecommons.org/licenses/by/4.0/>), which permits unrestricted use, distribution, and reproduction in any medium, provided the original author and source are credited.